

Photoproduction of η mesons on the deuteron above $S_{11}(1535)$ in the presence of a narrow $P_{11}(1670)$ resonance

A. Fix* and L. Tiator

Institut für Kernphysik, Johannes Gutenberg-Universität Mainz, D-55099 Mainz, Germany

M. V. Polyakov

Institut für Theoretische Physik II, Ruhr-Universität Bochum, D-44780 Bochum, Germany

(Dated: July 15, 2018)

Incoherent photoproduction of η -mesons on the deuteron is considered. The main attention is paid to the region above the $S_{11}(1535)$ resonance where rather narrow resonance like structure in the total cross section extracted for $\gamma n \rightarrow \eta n$ has been reported. The corresponding experimental results are analyzed from the phenomenological standpoint within the model containing a baryon P_{11} with the mass about 1670 MeV and a width less than 30 MeV. This resonance was suggested in some recent works as a nonstrange member of the pentaquark antidecuplet with $J^P = 1/2^+$. The calculation is also performed for the polarized and nonpolarized angular distributions of η mesons. In addition, we present our predictions for the cross sections of the neutral kaons and double pion photoproduction, where the same narrow $P_{11}(1670)$ resonance is assumed to contribute through the decay into $K^0\Lambda$ and $\pi\Delta$ configuration.

PACS numbers: 13.60.Le, 21.45.+v, 24.70.+s, 25.20.Lj

I. INTRODUCTION

During recent years there has been a considerable improvement of experimental and theoretical results for the production of η -mesons above the $S_{11}(1535)$ resonance region. Extensive and accurate data were obtained for the reaction $\gamma p \rightarrow \eta p$ and to a lesser extent for $\gamma d \rightarrow \eta np$. Furthermore, an amount of data is now available for η photoproduction on quasifree protons and neutrons, where the knocked-out nucleons are detected in coincidence with η -mesons. The energy region of a special interest corresponds to the excitation of the nucleon-like resonance identified in the Particle Data Group listing as $P_{11}(1710)$ and marked there by three stars. The first question with respect to this particle concerns its status. This resonance clearly seen by several partial wave analysis (PWA) groups, e.g. [1], but was not found in the GWU πN analysis [2, 3]. Another aspect is related to the distinct role of $P_{11}(1710)$ in the physics of pentaquarks. This state was assumed in [4] to be a nonstrange member of the antidecuplet representation ($\overline{10}$) of the pentaquark multiplet $qqqq\bar{q}$. This assumption was then used to scale the masses of $\overline{10}$ members, and thus was the most crucial input for further search of Θ^+ , the $S = +1$ member of this baryon group. At the same time, as it is discussed in [5] in this case a question arises, how to reconcile a small width of Θ^+ (less than 1 MeV according to the estimations noted in [5]) with rather broad structure of its presumable nonstrange partner $P_{11}(1710)$ (on average 100 MeV according to PDG [6]). As is emphasized in [5], this principal difference seems to contradict an expectation that the widths of particles entering the same multiplet should be comparable. Another problem with $P_{11}(1710)$ as a member of $\overline{10}$ is its too large mass. It is about 30 MeV larger than the value required by the Gell-Mann-Okubo rule [7], if one takes for the mass of $\Xi_{3/2}^-$, the heaviest member of $\overline{10}$, the value 1862 MeV reported in [8].

To resolve the discrepancy, it was suggested in Refs. [5, 7] that another P_{11} state has to be put on the place of a nonstrange $\overline{10}$ member. Like the $P_{11}(1710)$ this new state was assumed to be highly inelastic with the main nonstrange decay modes ηN and $\pi\Delta$. But contrary to $P_{11}(1710)$ it should have a smaller decay width $\Gamma_{P_{11}} \leq 10$ MeV and a lower mass $M \approx 1670$ MeV. A modified PWA analysis of πN [5], modified in such a way that it becomes more sensitive to baryons with smaller widths has shown that there are narrow regions in the baryon spectrum around 1680 and 1730 MeV where exotic states might exist. Moreover, as was shown in [9], due to the specific isotopic structure of the $\gamma N \rightarrow P_{11}$ transition, this resonance should be photoproduced mostly on a neutron rather than on a proton.

From the considerations above it is clear that a natural way to verify the theory of $\overline{10}$ is to look for a narrow structure in the energy dependence of the total cross section for photoproduction of η and other light mesons on neutrons. First steps in this direction were made in the experimental works of GRAAL [10], CB-ELSA [11, 12], and LNS-Tohoku [13] where the cross section for $\gamma n \rightarrow \eta n$ was extracted from the reaction on the deuteron. The preliminary data really seem to exhibit a peak around $E_\gamma = 1$ GeV what roughly corresponds to the γN invariant

* Permanent address: Laboratory of mathematical physics, Tomsk Polytechnic University, 634034 Tomsk, Russia

mass $W = 1670$ MeV, if one assumes the initial neutron to be at rest in the target.

The question about the nature of the observed peak was already touched upon on the phenomenological basis in [10, 14, 15]. The present paper is partially intended to provide a calculation of the reaction $\gamma d \rightarrow \eta np$ that would not suffer from different uncertainties, like the oversimplified treatment of the Fermi motion and final state interactions. Moreover we present the results for some asymmetries of this reaction in order to study their sensitivity to the possible contribution of a narrow P_{11} state.

Another point related to the P_{11} problem has a more practical aspect. It deals with the ratio σ_n/σ_p of the neutron to the proton cross section for η photoproduction around the lab photon energy 1020 MeV. This ratio measured for quasifree nucleons in [11, 12] exhibits a clear resonance behavior with the width about 100 MeV. A natural explanation of this phenomenon would be an existence of a baryon resonance which is predominantly excited on a neutron. In the EtaMAID model [16] this feature is assigned to $D_{15}(1675)$. The results of EtaMAID2001 for σ_n/σ_p give quite a good account of the data [11, 12]. However the problem with EtaMAID2001 is that the ηN decay width $\Gamma_{\eta N} \approx 0.17 \Gamma_{tot}$ needed to fit the data for $\gamma p \rightarrow \eta p$ is an order of magnitude larger than the value, suggested by the PDG listing (less than 1% of Γ_{tot}) and visibly exceeds the boundaries given by the $SU(3)$ analysis (about 3% of Γ_{tot}) [17, 18]. The latter discrepancy is especially unsatisfactory inasmuch as the $D_{15}(1675)$ state is a member of a well established baryon octet with branchings determined by the broken $SU(3)$ symmetry. This inconsistency was already discussed in [19]. It would therefore be interesting to see whether an inclusion of a hypothetic narrow $P_{11}(1670)$ baryon into the production amplitude instead of a too strong $D_{15}(1675)$ could provide a reasonable explanation of the structure seen in σ_n/σ_p . Although the nucleon-like member of $\bar{10}$ is assumed to be very narrow, the effect of broadening needed to fit the data might be due to Fermi motion in the deuteron.

In addition to the previous works where only the ηN channel was explored, we also pay some attention to kaon and double pion photoproduction. According to the results of [5] there is a non-vanishing probability for the exotic P_{11} to decay into $K\Lambda$ and $\pi\Delta$ states. For instance, the $\pi\Delta$ mode was estimated in [5] on the level of 30%. If the members of $\bar{10}$ are predominantly excited on a neutron, it is clear that from the experimental point of view, the easiest way to investigate the $P_{11} \rightarrow \pi\Delta$ transition is to measure the reaction $\gamma d \rightarrow \pi^- \pi^0 pp$. The other channels will contain strong proton contributions, and like in the η case this will lead to the necessity to single out the neutron reaction. So far in the region around $E_\gamma = 1$ GeV only one measurement of $\gamma d \rightarrow \pi^- \pi^0 pp$ was reported in [20], which furthermore has very large experimental uncertainties. Here we present our results for the corresponding total cross sections, where the role of $P_{11}(1670)$ in $\pi\pi$ and kaon photoproduction can be seen.

In section II we outline the model used for our calculation of $\gamma d \rightarrow \eta np$ and show our results for different channels and observables in section III. In section IV we close with a summary and conclusions.

II. FORMALISM

In this section we briefly review the formal ingredients of the quasifree η photoproduction on the deuteron

$$\gamma + d \rightarrow \eta + p + n. \quad (1)$$

Taking as independent variables the 3-momentum of the proton \vec{p}_p in the deuteron lab frame and the spherical angle Ω_{q^*} of the η -meson momentum \vec{q}^* in the ηn c.m. system, one obtains for the unpolarized cross section

$$\frac{d\sigma}{d\vec{p}_p d\Omega_{q^*}} = \frac{1}{6} \mathcal{K} \sum_{sm_s \lambda m_d} |\langle sm_s | \hat{T} | \lambda 1 m_d \rangle|^2, \quad (2)$$

where the phase space factor reads

$$\mathcal{K} = \frac{1}{(2\pi)^5} \frac{M_N^2}{4\omega_\gamma} \frac{|\vec{q}^*|}{E_p W_{\eta n}}. \quad (3)$$

In Eq. (3) ω_γ and E_p are the photon and the proton energies in the lab frame and M_N and $W_{\eta n}$ are the nucleon mass and the ηn invariant energy. The final state is determined by total spin (sm_s) of the NN system. The index λ denotes the photon polarization and ($1m_d$) stands for the deuteron spin.

As for the polarization observables, we considered only the asymmetries having counterparts in the elementary reaction $\gamma N \rightarrow \eta N$. Namely, we took the (linear) beam asymmetry Σ , the target asymmetry for vector polarized deuterons T_{11}^0 , and the beam-target asymmetry T_{10}^c for circularly polarized photons and vector polarized deuterons.

For their definitions we take the formulas similar to those obtained in Ref. [21]

$$\Sigma \frac{d\sigma}{d\Omega_{q^*}} = \frac{1}{3} \int d\vec{p}_p \mathcal{K} \sum_{sm_s m_d} T_{sm_s 1 m_d}^* T_{sm_s -1 m_d}, \quad (4)$$

$$T_{11}^0 \frac{d\sigma}{d\Omega_{q^*}} = \frac{2}{3} \int d\vec{p}_p \mathcal{K} \sum_{sm_s m_d} (T_{sm_s 1 -1}^* T_{sm_s 10} + T_{sm_s 10}^* T_{sm_s 11}), \quad (5)$$

$$T_{10}^c \frac{d\sigma}{d\Omega_{q^*}} = \int d\vec{p}_p \mathcal{K} \sum_{sm_s m_d} (|T_{sm_s 11}|^2 - |T_{sm_s 1 -1}|^2) \quad (6)$$

with $T_{sm_s \lambda m_d} = \langle sm_s | \hat{T} | \lambda 1 m_d \rangle$. Note that the last observable (6) differs by a factor $\frac{1}{\sqrt{6}}$ from that given in [21]. In this form it is equal to the familiar GDH integrand for the deuteron [22]. In a simpler form the corresponding formulas read

$$\Sigma \frac{d\sigma}{d\Omega_{q^*}} = \frac{1}{2} \frac{d\sigma_{\perp} - d\sigma_{\parallel}}{d\Omega_{q^*}}. \quad (7)$$

Here σ_{\perp} (σ_{\parallel}) is the cross section with the photon beam polarized perpendicular (parallel) to the reaction plane.

$$T_{11}^0 \frac{d\sigma}{d\Omega_{q^*}} = \frac{1}{2} \frac{d\sigma_{+} - d\sigma_{-}}{d\Omega_{q^*}}, \quad (8)$$

where σ_{+} (σ_{-}) corresponds to the target polarized "up" ("down") in the direction of $\vec{k} \times \vec{q}$. Finally, the spin asymmetry (6) reads

$$T_{10}^c \frac{d\sigma}{d\Omega_{q^*}} = \frac{d\sigma^P - d\sigma^A}{d\Omega_{q^*}}, \quad (9)$$

where $d\sigma^P$ and $d\sigma^A$ correspond to the photon spin oriented parallel and antiparallel to the deuteron spin. In the case of a free nucleon, the vector polarization T_{11}^0 corresponds to the target polarization T and the beam-target double polarization T_{10}^c corresponds to the polarization observable E . More precisely, if we neglect Fermi motion we get

$$T_{11}^0 \rightarrow -T \quad \text{and} \quad T_{10}^c \rightarrow -E. \quad (10)$$

The effect of Fermi motion can best be seen on the fact that in parallel kinematics the absolute value of the double polarization T_{10}^c is not exactly 1 as in the case of a free nucleon.

To construct the single nucleon operator for η photoproduction we use the η -MAID analysis developed in [16] and [23]. The resonance contribution in the partial wave α is parameterized in terms of standard Breit-Wigner functions

$$t_{\gamma, \eta}^{\alpha}(R; \lambda) = \tilde{A}_{\lambda} \frac{\Gamma_{tot} W_R}{W_R^2 - W^2 - i W_R \Gamma_{tot}} f_{\eta N}(W) \zeta_{\eta N}, \quad (11)$$

where a hadronic phase $\zeta_{\eta N} = \pm 1$ fixes a relative sign between the $N^* \rightarrow \eta N$ and the $N^* \rightarrow \pi N$ couplings. For most of the states the phases $\zeta_{\eta N}$ were treated as free parameters in the fitting procedure. As principal fit parameters of our analysis we used the resonance masses W_R , the total widths $\Gamma_R = \Gamma_{tot}(W_R)$, the branching ratios $\beta_{\eta N} = \Gamma_{\eta N}(W_R)/\Gamma_R$ and the photon couplings $\tilde{A}_{\lambda} = \{A_{1/2}, A_{3/2}\}$. However, we fix those parameters, where reliable results are given by PDG, see Tables I and II. For more details of the parametrization of the energy-dependent widths and the vertex function $f_{\eta N}(W)$ we would like to refer the reader to Refs. [16] and [23].

As mentioned above, the standard EtaMAID model [16] contains a too large contribution of $D_{15}(1675)$ which is inconsistent with rather small mean value of $\beta_{\eta N}$ given by PDG as well as with the $SU(3)$ symmetry bounds [18]. An alternative approach to $\gamma N \rightarrow \eta N$ was implemented in [23] where the experimentally observed increase of η production on the proton in the forward direction is reproduced by Regge poles in the t channel. In this case the contribution of D_{15} can be weakened down to 0.7% in accordance to the PDG analysis. At the same time, as will be discussed in the next section, this model being fitted to the proton data cannot account for the preliminary results of $\gamma n \rightarrow \eta n$, where the calculated cross section in the region $E_{\gamma} > 900$ MeV exhibit a smooth energy dependence, whereas the data show a pronounced peak.

In the present paper we consider two models for $\gamma N \rightarrow \eta N$: (i) the standard EtaMAID model [16], with strong coupling of $D_{15}(1675)$ to the ηN state ($\Gamma_{\eta N} = 0.17 \Gamma_{tot}$), and (ii) the modified reggeized MAID model [23] in which an additional narrow P_{11} state is inserted. The parameters of the P_{11} resonance are listed in Table III. For the total

TABLE I: Parameters of nucleon resonances from EtaMaid2001 [16] with standard vector meson poles, model (I). The masses and widths are given in MeV, $\beta_{\eta N}$ is the branching ratio for the eta decay channel and $\zeta_{\eta N}$ the relative sign between the $N^* \rightarrow \eta N$ and the $N^* \rightarrow \pi N$ couplings. The photon couplings to the proton and neutron target for helicity $\lambda=1/2$ and $3/2$ are given in units of $10^{-3}/\sqrt{\text{GeV}}$. The underlined parameters are fixed and are taken from PDG [6]. The asterisk for $nA_{1/2}$ of the $S_{11}(1535)$ denotes a fixed n/p ratio obtained from the threshold experiment[24].

N^*	Mass	Width	$\beta_{\eta N}$	$\zeta_{\eta N}$	$pA_{1/2}$	$pA_{3/2}$	$nA_{1/2}$	$nA_{3/2}$
$D_{13}(1520)$	<u>1520</u>	<u>120</u>	0.06%	+1	-52	<u>166</u>	<u>-41</u>	<u>-135</u>
$S_{11}(1535)$	1541	191	<u>50%</u>	+1	118	—	-97*	—
$S_{11}(1650)$	1638	114	8%	-1	68	—	-56	—
$D_{15}(1675)$	1665	<u>150</u>	17%	-1	18	24	<u>-43</u>	<u>-58</u>
$F_{15}(1680)$	1682	<u>130</u>	0.06%	+1	-21	124	<u>52</u>	<u>-41</u>
$D_{13}(1700)$	<u>1700</u>	<u>100</u>	0.3%	-1	<u>-18</u>	<u>-2</u>	<u>0</u>	<u>-3</u>
$P_{11}(1710)$	1720	<u>100</u>	26%	+1	23	—	<u>-2</u>	—
$P_{13}(1720)$	<u>1720</u>	<u>150</u>	3%	-1	<u>18</u>	<u>-19</u>	<u>1</u>	<u>-29</u>

TABLE II: Parameters of nucleon resonances from EtaMaid2003 [23] with reggeized vector mesons, model (II). Notation as in Table I.

N^*	Mass	Width	$\beta_{\eta N}$	$\zeta_{\eta N}$	$pA_{1/2}$	$pA_{3/2}$	$nA_{1/2}$	$nA_{3/2}$
$D_{13}(1520)$	<u>1520</u>	<u>120</u>	0.04%	+1	<u>-24</u>	<u>166</u>	<u>-59</u>	<u>-139</u>
$S_{11}(1535)$	1521	118	<u>50%</u>	+1	80	—	-65*	—
$S_{11}(1650)$	1635	120	16%	-1	<u>46</u>	—	<u>-38</u>	—
$D_{15}(1675)$	1665	<u>150</u>	0.7%	+1	19	15	<u>-43</u>	<u>-58</u>
$F_{15}(1680)$	1670	<u>130</u>	0.003%	+1	-15	133	<u>29</u>	<u>-33</u>
$D_{13}(1700)$	<u>1700</u>	<u>100</u>	0.025%	-1	<u>-18</u>	<u>-2</u>	<u>0</u>	<u>-3</u>
$P_{11}(1710)$	1700	<u>100</u>	26%	-1	<u>9</u>	—	<u>-2</u>	—
$P_{13}(1720)$	<u>1720</u>	<u>150</u>	4%	+1	<u>18</u>	<u>-19</u>	<u>1</u>	<u>-29</u>

width we use two values $\Gamma_{tot}(P_{11}) = 10$ MeV and $\Gamma_{tot}(P_{11}) = 30$ MeV. The former was found in Ref. [5] taking the octet-antidecuplet mixing angle from [4]. As is noted in [5] more recent information about this parameter points to a larger value of $\Gamma_{\pi\Delta}(P_{11})$ which might result in an increasing total P_{11} width up to ~ 30 MeV. Furthermore, as pointed out in [5] this latter value should be an upper bound of the resonance width treated as undetectable in their modified πN PWA. The neutron photocoupling of $P_{11}(1670)$ is chosen according to the phenomenological analysis of Ref. [14] and the chiral quark-soliton model calculations of Ref. [25].

To calculate the cross section on the deuteron we use a production operator valid in an arbitrary frame of reference. For this purpose we resort to the standard scheme to pass from the CGLN amplitudes F_i to the Lorentz invariant amplitudes A_i (see, e.g., [26, 27]). The effects of final state interaction (FSI) were included within a method where rescatterings within the pairs of particles are taken into account up to the first order in the corresponding two-body t -matrices. In general we have

$$\hat{T} = \hat{T}^{IA} + \hat{T}^{NN} + \hat{T}^{\eta N}, \quad (12)$$

where the first term on the r.h.s. stands for the impulse approximation, which for the noncoherent reaction is equivalent to the spectator nucleon model. The terms T^{NN} and $T^{\eta N}$ include one-loop NN and ηN rescattering mechanisms as is explained in [28]. The operator \hat{T}^{IA} can schematically be presented as a sum of the elementary operators referring

TABLE III: Mass, total width, ηN branching ratio and photon helicity couplings in units of $(10^{-3}/\sqrt{\text{GeV}})$ for the P_{11} pentaquark state in our calculation.

Mass	Width	$\beta_{\eta N}$	$\beta_{\pi\Delta}$	$\beta_{K\Lambda}$	$pA_{1/2}$	$nA_{1/2}$
1670	10(30)	40%	30%	30%	8	30(35)

to a proton and a neutron

$$\hat{T}^{IA} = \hat{t}_p(1) + \hat{t}_n(2), \quad (13)$$

where $\hat{t}(i)$ acts on the i th nucleon. The actual results, e.g. for a quasifree neutron, are obtained by setting $\hat{t}_p = 0$ in the expression (13). The last two terms in Eq. (12) contain interaction between the corresponding particles. For formal details, concerning the treatment of FSI effects in $\gamma d \rightarrow \eta np$ we refer the reader to Ref. [28].

III. RESULTS AND DISCUSSION

Before going to the details it is instructive to estimate possible contributions of $P_{11}(1670)$ into different channels. For this purpose we use the formula which gives the partial cross section at the resonance position $W = W_R$

$$\sigma_X = \xi_X(2J+1) \frac{\pi}{\omega_\gamma^2} \frac{\Gamma_{\gamma N^*} \Gamma_{N^* \rightarrow X}}{\Gamma_{tot}^2}, \quad X \in \{\eta n, \pi\pi n, K^0\Lambda\}. \quad (14)$$

Here the factor ξ_X ($0 < \xi_X \leq 1$) takes into account isotopic separation of the $N^* \rightarrow X$ vertex. In particular one obtains

$$\xi_{\eta n} = \xi_{K^0\Lambda} = 1, \quad \xi_{\pi^+\pi^-n} = 5/9, \quad \xi_{\pi^-\pi^0n} = \xi_{\pi^0\pi^0n} = 2/9. \quad (15)$$

Taking $J = 1/2$ and the $P_{11}(1670)$ helicity amplitudes as well as the widths from Table III (for a moment we take $\Gamma_{tot}(P_{11}) = 10$ MeV) we will have at the resonance point $W = W_R$

$$\sigma_{\eta n} \approx 15 \mu b, \quad \sigma_{\pi^+\pi^-n} \approx 6.7 \mu b, \quad \sigma_{\pi^-\pi^0n} = \sigma_{\pi^0\pi^0n} \approx 2.7 \mu b, \quad \sigma_{K^0\Lambda} \approx 11 \mu b. \quad (16)$$

The so obtained P_{11} partial cross sections have to be compared to the characteristic values of the corresponding total cross sections in the region $E_\gamma \approx 1020$ MeV

$$\sigma_{\eta n} \approx 13 \mu b [16], \quad \sigma_{K^0\Lambda} \approx 2.5 \mu b [29], \quad (17)$$

$$\sigma_{\pi^+\pi^-n} \approx 70 \mu b [30], \quad \sigma_{\pi^-\pi^0n} \approx 40 \mu b [30], \quad \sigma_{\pi^0\pi^0n} \approx 4 \mu b [30]. \quad (18)$$

Thus, already these simple estimations show that the channel ηn provides the largest value of the ratio ($\sigma_X/\text{background}$) and might be the most favorable. In other channels the signal from P_{11} is expected to be quite weak.

We continue our discussion turning to the total cross section of $\gamma d \rightarrow \eta np$ shown in Fig. 1 as a function of the photon laboratory energy. Firstly, it demonstrates the influence of the final state interaction (FSI) which is visualized as a scattering of the produced particles in the two-body subsystems NN and ηN . As is explained in [28] the effect is essential in the region $E_\gamma < 700$ MeV, so that its inclusion is absolutely necessary to restore the agreement with the low-energy data [24]. In the vicinity of the $S_{11}(1535)$ peak the FSI effect mostly comes from the absorption of the produced η mesons on the deuteron through the transition to pions. This situation is quite typical for reactions proceeding through the resonance excitation. For heavier nuclei it results in a strong absorption rate [31], so that the interaction of the produced η -mesons with the target is predominantly of a diffractive character. Clearly, in our case this effect is softened by a small number of nucleons in the deuteron. With increasing energy the influence of FSI vanishes, so that the IA should be considered as a good approximation to the reaction dynamics. This result is quite foreseeable, since both NN and ηN interaction are important almost exclusively in the s -waves which occupy only a very small fraction of the phase space available at high energies. The influence of FSI becomes more visible in the η angular distribution presented on the right panel of Fig. 1. However, the general validity of IA shows that our notion about the process on the deuteron as the one taking place on one of the nucleons with another nucleon mainly behaving as a spectator is justified.

In Fig. 2 we show our results for the total cross section on quasifree nucleons calculated within the strong D_{15} approach (i) and the narrow P_{11} model (ii). In the same figure the dashed lines are the corresponding single nucleon cross sections. Firstly, as we can see, the Fermi motion strongly influences the parameters of the P_{11} peak. Namely its width becomes about 7 times larger in comparison to the free nucleon, whereas its position remains unchanged. In this context we also note that even though the peak observed in [11, 12] is quite narrow, the width $\Gamma_{tot}(P_{11}) = 10$ MeV seems to be somewhat too small in order to fit the experimental results. If we change from 10 MeV to 30 MeV the agreement with the CB-ELSA data is improved.

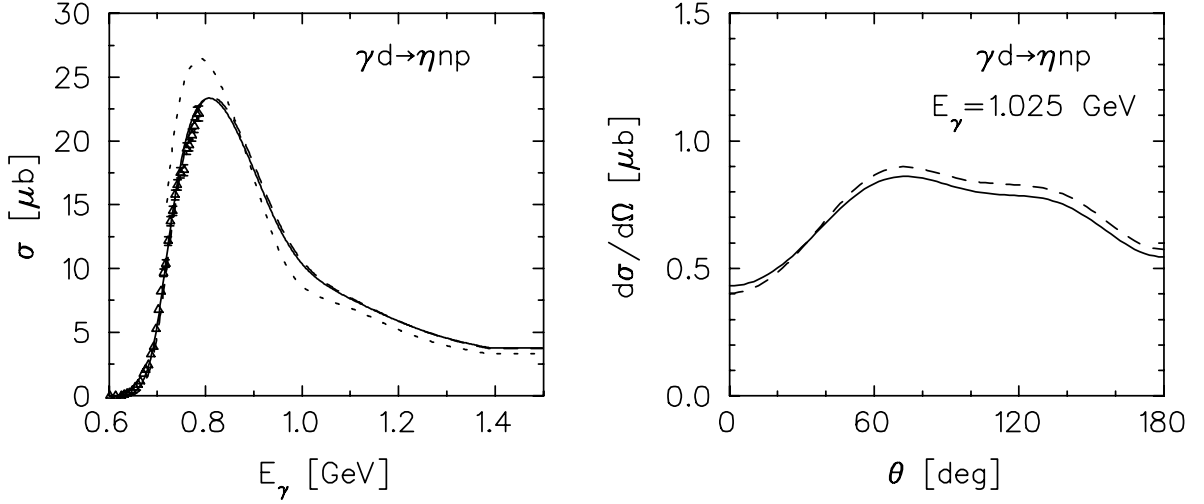


FIG. 1: Left panel: total cross section for $\gamma d \rightarrow \eta np$. Right panel: η angular distribution for $\gamma d \rightarrow \eta np$ calculated in the ηn c.m. frame. The dashed curves show the results of the impulse approximation and the solid curves include interaction between the final particles. The dotted curve on the left panel is the sum of the total cross sections on the free proton and neutron. For the elementary amplitude the EtaMaid2001 model [16] is used. The data points are from Ref. [24].

It is interesting that although the model (i) does not reproduce the shape of the quasifree neutron cross section around $E_\gamma \approx 0.9$ GeV (left upper panel in Fig. 2), it gives quite a good description of the rapidly varying quantity σ_n/σ_p presented on the right panel. Analyzing the energy dependence of σ_n and σ_p one can conclude that a narrow structure in this ratio is primarily due to a shoulder in the proton cross section. It becomes less distinct in the deuteron, because of filling the slight minimum in σ_p at $E_\gamma = 1$ GeV, what should be a natural consequence of a smearing effect caused by the Fermi motion. As a result, the theoretical ratio σ_n/σ_p turns down from 1.4 to about 1.2. At the same time, it is somewhat strange that this natural change is not supported by the preliminary experimental results [12] (filled circles in the middle panels). The latter remain to be better described by the MAID calculation for a free proton.

As is shown in Fig. 1 the model predicts a visible modification of the form and the height of the $S_{11}(1535)$ peak when we pass from the free nucleon to the bound nucleon in the deuteron. The main reason is that the phase space factor \mathcal{K} for three particles (3) increases more slowly than the two-body phase space in the elementary process. As a result, the resonance form of the amplitude folded by \mathcal{K} is slightly shifted to the right on the energy scale. In the vicinity of $P_{11}(1670)$, where the effects caused by the mass difference between the nucleon and the deuteron become insignificant, the peak position in the reaction on a deuteron nearly coincide with the one on the free nucleon.

As we can see from Fig. 2 our calculation with $A_{1/2}^p \approx \frac{1}{3} A_{1/2}^n$ predicts quite a pronounced peak also in the total cross section on a free proton. In this connection it seems to be reasonable to analyze the available data for $\gamma p \rightarrow \eta p$ [32, 33, 34, 35] using finer energy binning in the corresponding energy region. As an example we plotted in Fig. 3 our predictions for the $d\sigma/d\Omega_{q^*}$ and Σ asymmetry for three different η angles in ηN c.m. system. In particular, the results show that the nonpolarized cross section is more sensitive to the P_{11} contribution in the backward angular region, whereas in the beam asymmetry this resonance should be visible in both hemispheres.

As already noted, while both reaction mechanisms (i) and (ii) give similar results for the total cross section, due to the different orbital momentum of the D_{15} and P_{11} resonances, they will show up with different angular distributions. This difference is clearly seen in Fig. 4, where we show our calculations for a neutron at $E_\gamma = 1020$ MeV for a) the strong D_{15} model (i), b) the narrow P_{11} model (ii) with a phase $\zeta_{\eta N} = +1$ and c) the narrow P_{11} model (ii) with a phase $\zeta_{\eta N} = -1$. In the angular distribution the hadronic phase becomes important, since the P_{11} partial wave interferes with other partial waves like the S_{11} . In the total cross section it can only interfere with other contributions in the same partial wave, e.g. from the background, and the difference can hardly be seen. As we can see the model (ii) predicts quite a weak linear dependence of the unpolarized cross section, what is obviously explained by the dominance of the electric E_{0+} and magnetic M_{1-} dipole amplitudes. In the ideal case of only S_{11} and P_{11} partial waves one obtains

$$d\sigma/d\Omega \sim |E_{0+}|^2 + |M_{1-}|^2 - 2\text{Re}(E_{0+}^* M_{1-}) \cos \theta. \quad (19)$$

For S_{11} and D_{15} we have a more complicated angular dependence which is symmetric with respect to $\cos \theta = 0$

$$d\sigma/d\Omega \sim A + B \cos^2 \theta + C \cos^4 \theta, \quad (20)$$

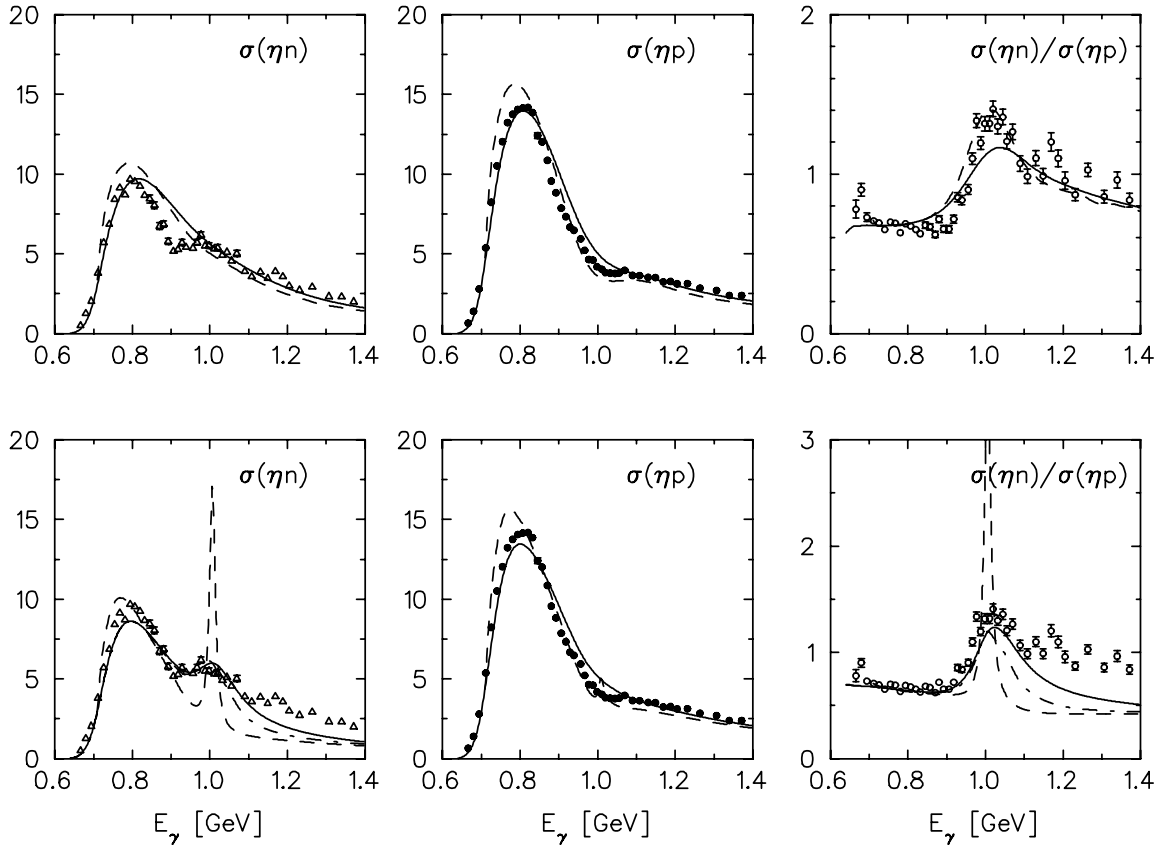


FIG. 2: Total cross section for noncoherent η photoproduction on a deuteron versus the photon lab energy. The results are presented for the strong D_{15} model (i) (upper row) and the narrow P_{11} model (ii) (lower row). The dashed curves show the corresponding single nucleon cross sections. The dash-dotted and the solid curves on the left and the right panels in the lower row are obtained with $\Gamma_{P_{11}} = 10$ MeV and $\Gamma_{P_{11}} = 30$ MeV respectively. The free nucleon cross section corresponds to $\Gamma_{P_{11}} = 10$ MeV. The preliminary data from Ref. [12] are normalized to the EtaMAID calculations in the first maximum.

where the coefficients A, B , and C are quadratic forms of the multipoles E_{0+} , E_{2+} , and M_{2+} . Of course, in the real situation the observed cross section can not be explained entirely by only two resonances so that this ideal picture is distorted by the presence of other, less important, states with different quantum numbers.

In the same figure we demonstrate angular distributions of η -mesons, obtained with polarized photon beam and target. As already noted, for the polarization observables we took only those, which can easily be interpreted for quasifree reactions. The photon asymmetry Σ given by the strong D_{15} model (i) visibly overestimates that provided by the narrow P_{11} model. In the extreme case of pure D_{15} amplitude we will have $\Sigma(\theta = 90^\circ) = 1$. On the contrary, in the model (ii) the nontrivial Σ asymmetry is only due to interference of the S_{11} and the P_{11} waves with higher spin states. The same is true for the vector target asymmetry T_{11}^0 . Here again the model (i) demonstrates typical D_{15} behavior with strong rise at forward angles and crossing zero close to $\theta = 90^\circ$. The model (ii) gives the nonzero value of T_{11}^0 due to interference of the dominating resonances S_{11} and P_{11} with other resonance states having $J > 1/2$. The last asymmetry is therefore relatively small and should be more model dependent. The angular distribution shown by the GDH-asymmetry T_{10}^c is what one could expect from the results for the nonpolarized cross section on the left upper panel. Here the model (ii) with the dominating $S_{11} + P_{11}$ mode contributes only to the antiparallel component $d\sigma^A$ in (6). As a consequence, one sees about the doubled value of the corresponding nonpolarized cross section in accordance with the definition (6), which again exhibits quite a weak angular dependence. The D_{15} resonance gives a strong parallel component $d\sigma^P$, so that the resulting asymmetry qualitatively reproduces the unpolarized angular distribution with two distinct peaks.

As for the other channels $\pi\pi$ and $K\Lambda$, here the situation is less clear. According to our estimates at the beginning of this section, these channels seem to be not so effective as a tool to detect $P_{11}(1670)$. As an example, in Fig. 5 we present our predictions for the corresponding cross sections. In the $\pi\pi$ case the corresponding signal is rather weak. Moreover, the differential cross section could be difficult to analyze, since there are too many parameters involved. In the charged channels the angular distribution at such a high energy is mostly localized in the forward direction.

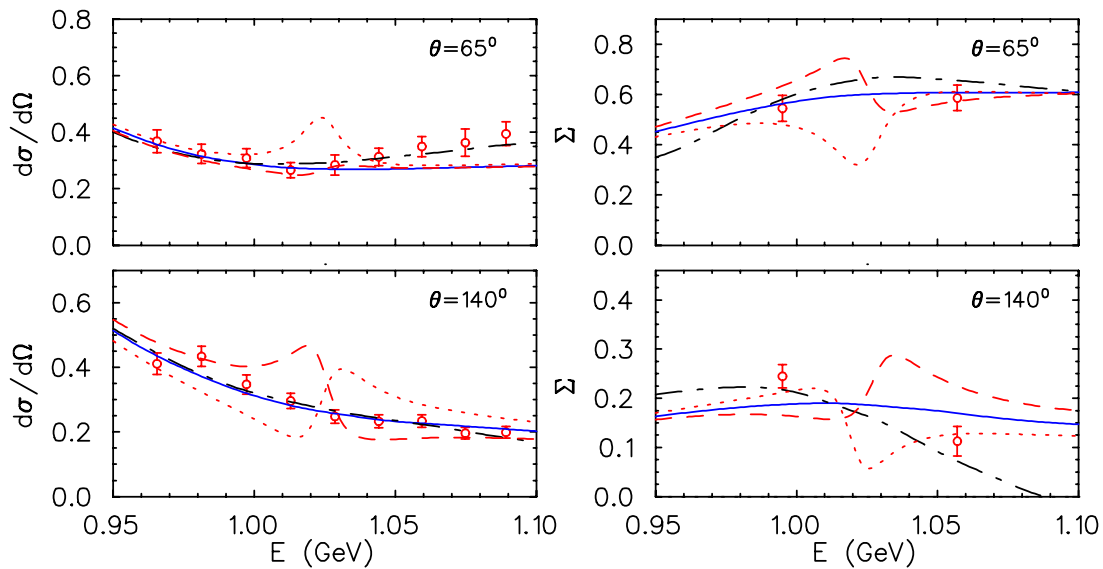


FIG. 3: Differential cross section and beam asymmetry for η photoproduction on a free proton. The solid and the dash-dotted curves are calculated with the Reggeized model [23] (without $P_{11}(1670)$) and the ordinary EtaMAID model (i) [16]. Addition of the narrow P_{11} resonance with $\zeta_{\eta N} = +1(-1)$ into the Reggeized amplitude gives the dashed (dotted) curve. The data are from GRAAL, Ref. [32] for the cross section and Ref. [36] for the beam asymmetry.

This is due to dominance of the pion contact term, where a virtual pion becomes a real one by the coupling of the photon with the pion current. Clearly the importance of this peripheral mechanism makes the angular distribution more difficult to interpret in terms of low powers of $\cos \theta$.

In the neutral channel $\gamma d \rightarrow \pi^0 \pi^0 n p$ the cross section is more sensitive to resonance contributions. However, the corresponding angular distribution turns out to be symmetric with respect to $\cos \theta = 0$ regardless of the parity of the resonances which contribute. This is a trivial consequence of the identity of the produced pions and thus the corresponding analysis can hardly be useful. Furthermore, according to the results of Ref. [30], in the region of 1 GeV the important role might be played by the excitation of $F_{15}(1680)$, so that P_{11} or D_{15} seem to be much less important. In K^0 photoproduction the peak although being more visible is located just on the top of the slope and therefore could be difficult for experimental identification.

We recall that the calculation presented in Fig. 5 is performed under the assumption that $P_{11}(1670)$ decays with almost equal probabilities into all three channels ηN , $\pi \Delta$, and $K \Lambda$ (see Table III). Therefore, if the partial widths will be better known in the future, the height of the peaks in Fig. 5 as well as in Fig. 2 could easily be scaled using, e.g., the formula (14). However, we can expect that our qualitative conclusion about the preference of the ηN channel as a tool to study a P_{11} resonance will hardly be changed, until its mode remains on a level of more than 10-20 %.

IV. CONCLUSION

We have calculated photoproduction of η mesons in the region above the $S_{11}(1535)$ resonance, where an unusually narrow structure has been observed in recent experiments for $\gamma n \rightarrow \eta n$ on quasifree neutrons in a deuteron [10, 11, 12, 13]. One of our main objectives was to investigate the impact of Fermi motion and FSI on the elementary process $\gamma N \rightarrow \eta N$. From the presented studies we are confident that the description within the spectator model is good in the entire region overlapping $P_{11}(1670)$. As it is shown the corrections from the FSI are on the percent level so that the parameters of the single nucleon cross section can be deduced directly from the data. The Fermi motion effect results in essential smearing of a narrow structure in the cross section, like peaks and shoulders, what in some important cases leads to visible changes in the reaction characteristics. Altogether, we find that the presence of an exotic narrow resonance with a width about 10-30 MeV can explain the CB-ELSA data [11, 12].

In a recent paper of [37] another mechanism based on the strong contribution of $P_{11}(1710)$ to $\gamma n \rightarrow \eta n$ was considered. The authors showed that the bump structure in the cross section can be explained in terms of $S_{11}(1650) + P_{11}(1710)$ contributions without resorting to an exotic narrow $P_{11}(1670)$ state considered in the present paper. In this respect we note that according to the PDG analysis [6] as well as to the parameter set presented in [37] both $S_{11}(1650)$ and $P_{11}(1710)$ are coupled more strongly to γp than to γn . Therefore, it is reasonable to expect that

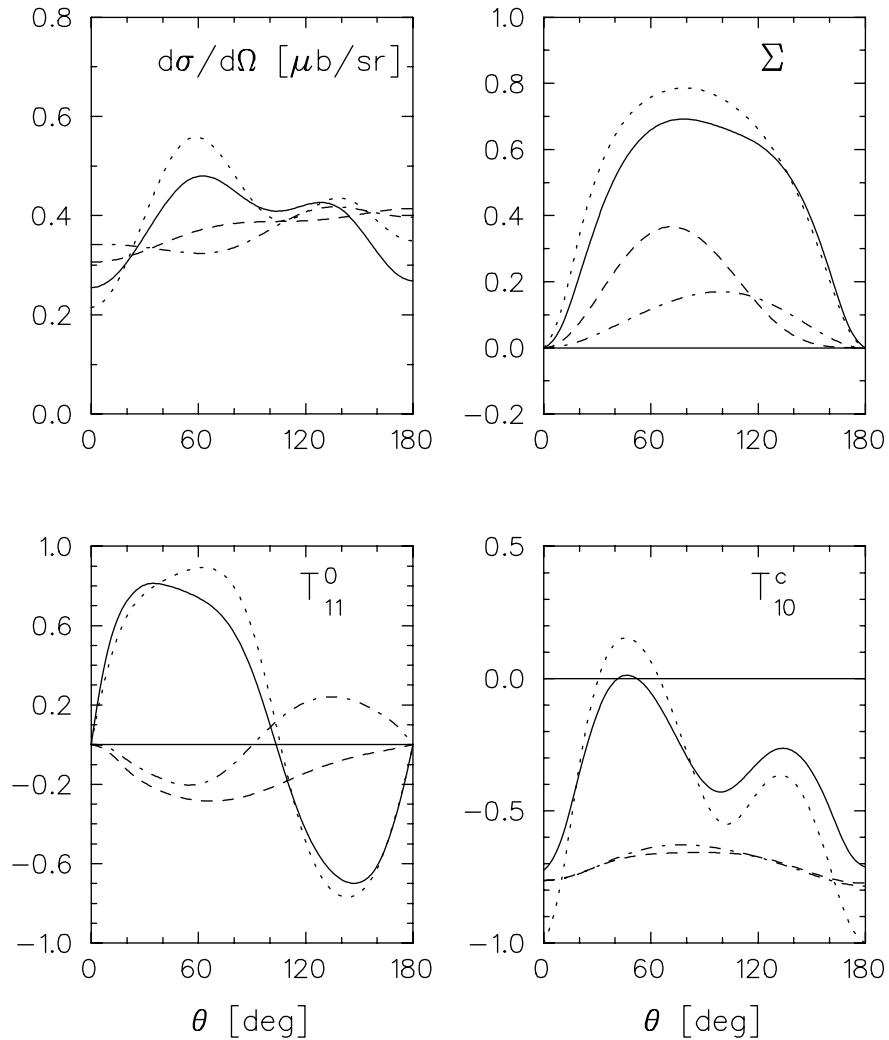


FIG. 4: Unpolarized differential cross section and spin asymmetries for η photoproduction on a quasifree neutron in a deuteron calculated at $E_\gamma = 1020$ MeV. The solid curves show the results of EtaMAID2001 with standard vector meson poles and a strong $D_{15}(1675)$ resonance. The dashed (dash-dotted) curves show the results with the reggeized model and a narrow $P_{11}(1670)$ resonance with a hadronic phase $\zeta_{\eta N} = +1(-1)$. The dotted lines show the observables on a free neutron, where $T_{11}^0 \rightarrow -T$ and $T_{10}^c \rightarrow -E$. The asymmetries are defined in Eqs. (4) to (6).

the same mechanism will produce even more pronounced bump in the cross section for $\gamma p \rightarrow \eta p$ which is however not experimentally observed. In the present paper we suggested another explanation. Namely, our purpose was to assign the structure to a narrow P_{11} state, which (i) is in accord with the chiral-soliton model [4], (ii) has a strong photocoupling to a neutron, and (iii) could elude identification in PWA due to its small width.

Another point to discuss is whether the available data reveal a true resonance in the reaction on a neutron at $E_\gamma = 1020$ MeV. As is seen from Fig. 2 crucial is the behavior of the cross section at 930 MeV, where according to the CB-ELSA results there is clear minimum. If we assume for the moment, that the minimum vanishes in the improved data analysis, then we will see only a wide structure. It might appear as a resonance in the σ_n to σ_p ratio simply because of slight minimum exhibited by the proton cross section at $E_\gamma = 1020$ MeV. Therefore, more general question concerning the experimental results for $\gamma n \rightarrow \eta n$ is why the neutron cross section is so high above the $S_{11}(1535)$ region, as compared to what we see on the proton. It is quite unlikely that here we deal with the interference of the resonances with the nonresonant background. The latter seems to be insignificant in η photoproduction, primarily due to the smallness of the ηNN coupling [38]. Among the known resonances there are (according to PDG) no states predominantly excited on a neutron and, at the same time, having a sufficiently large ηN branching ratio. Therefore, even if future investigations do not support the existence of a narrow $P_{11}(1670)$, the question about the nature of the η photoproduction on the neutron (and eventually on the proton) above the S_{11} will remain open.

As is noted in [5] it is a small width that can be used as a sign that the resonance particle, observed e.g. in meson

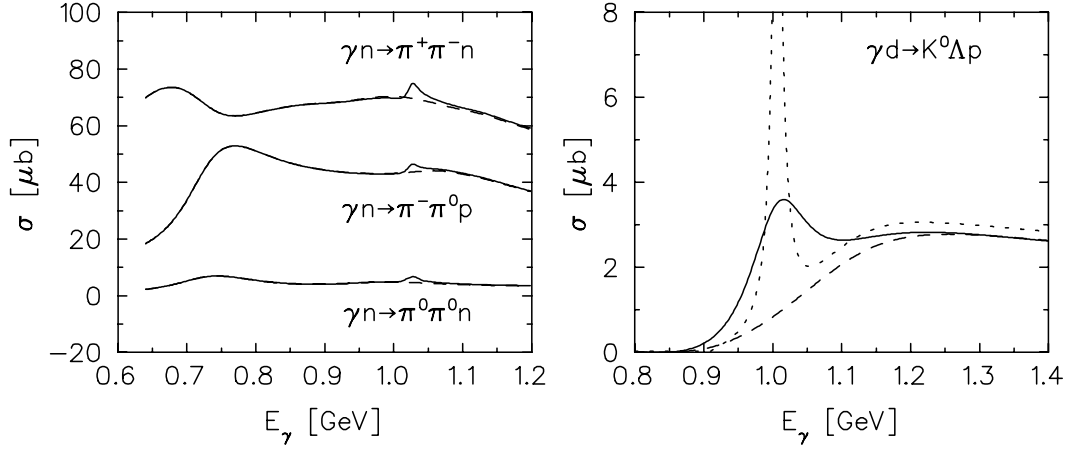


FIG. 5: Total cross section for $\gamma n \rightarrow \pi\pi N$ and $\gamma d \rightarrow K^0\Lambda p$. Dashed and solid curves are obtained with and without a narrow $P_{11}(1670)$ resonance. The dash-dotted curve on the right panel is the corresponding free neutron cross section.

production should be attached to the $\overline{10}$ group of baryons and not to the ordinary baryon octet (in the case of $\overline{10} \otimes 8$ mixture we can speak about dominating antidecuplet part in the particle wave functions). However it should be noted that if, for example, the analysis of the partial waves points to the dominance of an $S_{11} + P_{11}$ configuration in the $\gamma n \rightarrow \eta n$ amplitude it could be quite difficult to distinguish between the 'usual' P_{11} with its typical hadronic width of 100 MeV and an exotic narrow state P_{11} from $\overline{10}$. As the calculation shows the Fermi motion strongly smears the narrow resonance structure, so that in both cases we see a broad peak. Therefore, it is to expect that no simple test exists for discrimination between the 'ordinary' and exotic P_{11} resonances.

Acknowledgment

We thank V. Kuznetsov for providing us with GRAAL data, B. Krusche and I. Jaegle for the preliminary CB-ELSA data and I. Strakovsky for many helpful discussions. The work was supported by the Deutsche Forschungsgemeinschaft (SFB 443). M.V.P. is supported by the Sofja Kowalewskaja Programme of the Alexander von Humboldt Foundation.

-
- [1] G. Höhler, in *Pion-nucleon scattering*, Vol. I/9b2, Springer, Berlin 1983.
 - [2] R. A. Arndt, W. J. Briscoe, I. I. Strakovsky, R. L. Workman, and M. M. Pavan, Phys. Rev. C 69, 035213 (2004).
 - [3] R. A. Arndt, W. J. Briscoe, I. I. Strakovsky and R. L. Workman, Phys. Rev. C 74, 045205 (2006).
 - [4] D. Diakonov, V. Petrov, and M. Polyakov, Z. Phys. A 359, 305 (1997).
 - [5] R. A. Arndt, Ya. I. Azimov, M. V. Polyakov, I. I. Strakovsky, and R. L. Workman, Phys. Rev. C 69, 035208 (2004).
 - [6] W. M. Yao *et al.* [Particle Data Group], J. Phys. G 33, 1 (2006).
 - [7] D. Diakonov and V. Petrov, Phys. Rev. D 66 010001 (2002).
 - [8] C. Alt *et al.*, Phys. Rev. Lett. 92, 042003 (2004).
 - [9] M. V. Polyakov and A. Rathke, Eur. Phys. J. A 18, 691 (2003).
 - [10] V. Kouznetsov, hep-ex/0606065
 - [11] I. Jaegle, Proc. of the NSTAR2005 workshop, Tallahassee, FL, USA, 2005, World Scientific 2006, p. 340 and I. Jaegle, private communication.
 - [12] B. Krusche *et al.*, Proc. of the 4th Int. Conf. on Quarks and Nuclear Physics, Madrid, June 2006.
 - [13] J. Kasagi, Talk at Yukawa International Seminar YKIS2006, Kyoto, Japan, November-December 2006, <http://www2.yukawa.kyoto-u.ac.jp/~ykis06/>.
 - [14] Ya. Azimov, V. Kouznetsov M. V. Polyakov, and I. Strakovsky, Eur. Phys. J. A 25, (2005).
 - [15] K. S. Choi, S. i. Nam, A. Hosaka and H. C. Kim, Phys. Lett. B 636 (2006) 253.
 - [16] W.-T. Chiang, S. N. Yang, L. Tiator and D. Drechsel, Nucl. Phys. A 700, 429 (2002).
 - [17] N. P. Samios, M. Goldberg and B. T. Meadows, Rev. Mod. Phys. 46, 49 (1974).
 - [18] V. Guzey and M. V. Polyakov, hep-ph/0512355.
 - [19] L. Tiator, Proc. of the Meson2006 Workshop, Cracow, Poland, September 2006, nucl-th/0610114.
 - [20] R. Shiffer *et al.*, Nucl. Phys. B 38, 628 (1972).
 - [21] H. Arenhövel and A. Fix, Phys. Rev. C 72, 064004 (2005).

- [22] H. Arenhövel, A. Fix, and M. Schwamb, Phys. Rev. Lett. 93, 202301 (2004).
- [23] W.-T. Chiang, S. N. Yang, L. Tiator, M. Vanderhaeghen and D. Drechsel, Phys. Rev. C 68, 045202 (2003).
- [24] B. Krusche *et al.*, Phys. Lett. B 358, 40 (1995).
- [25] H. C. Kim, M. Polyakov, M. Praszalowicz, G. S. Yang and K. Goeke, Phys. Rev. D 71, 094023 (2005).
- [26] C. Bennhold and H. Tanabe, Nucl. Phys. A 530, 625 (1991).
- [27] B. Pasquini, D. Drechsel, and L. Tiator, Eur. Phys. J. A 27, 231 (2006).
- [28] A. Fix and H. Arenhövel, Z. Phys. A359, 427 (1997).
- [29] F. X. Lee, T. Mart, C. Bennhold, H. Haberzettl, L. E. Wright, Nucl. Phys. A 695, 237 (2001).
- [30] A. Fix and H. Arenhövel, Eur. Phys. J. A 25, 115 (2005).
- [31] M. Roebig-Lanadau *et al.*, Phys. Lett. B 373, 45 (1996).
- [32] F. Renard *et al.*, Phys. Lett. B 528, 215 (2002).
- [33] M. Dugger *et al.*, Phys. Rev. Lett. 89, 222002 (2002).
- [34] V. Crede *et al.*, Phys. Rev. Lett. 94, 012004 (2005).
- [35] T. Nakabayashi *et al.*, Phys. Rev. C 74, 035202 (2006).
- [36] V. Kouznetsov, *et al.*, πN Newsletters 16, 160 (2002).
- [37] V. Shklyar, H. Lenske and U. Mosel, nucl-th/0611036.
- [38] L. Tiator, C. Bennhold and S. S. Kamalov, Nucl. Phys. A 580, 455 (1994).